Virtual Concept International Workshop (VC-IW'14)
"Innovation on Product Design and Manufacturing". Medellín, Colombia

Graphs of Optimally Fit Features in Assessment of Geometric Tolerances

Oscar E. Ruiz[1], John Congote[1], Diego A. Acosta[2]

(1) **:** Universidad EAFIT, COLOMBIA
Laboratory of CAD CAM CAE
+57-4-2619500 / +57-4-2664284
E-mail : {oruiz,jcongote}@eafit.edu.co

(2) **:** Universidad EAFIT
DDP Group
+57-4-2619500 / +57-4-2664284
E-mail : dacostam@eafit.edu.co

Short Abstract: This article presents an industrial application case of geometric constraint graphs, whose nodes are statistically optimal instances of manufacturing or design features and whose edges are usual geometric relations used in tolerance applications. The features might be virtual ones. As a consequence, they may lie beyond the piece's extents. The geometric constraint graph may have cyclic topology. Contrary to deterministic geometric constraint graphs, tolerance constraint graphs admit numerical slacks, due to their stochastic nature. The methodology has been applied in industrial scenarios, showing superiority to traditional material features for the assessment of tolerances.

Key words: tolerance graphs, optimal fit, geometric constraints, datum, stochastic geometry

1- Introduction

In industrial applications, tolerance assessment must be conducted considering geometric constrains among features of: (i) the same body, and (ii) different bodies. This article refers to scope (i) above. It must be said, however, that constraint graphs apply to both steps, and geometric constraints are central to any application in design and manufacturing. In particular, in Parametric Tolerance systems, graphs of geometric constraints are fundamental ([DQ1]).

2- Literature Review

[SS1] considers plane and line fitting to point samples giving different weights to each point. We deal with cylinders, cones, and ellipsoids, besides planes and straight lines. [S1] is an overview of computational tolerance issues. For our purposes, we use, for example, Least Squares (as opposed to Chebyshev) fitting. In [S1], we can recognize that primitive fitting is still an open issue in Computational Tolerancing. [PSRS1] presents multidimensional SF (Substitute Features) fit to (semi) analytical forms. In the multidimensional domain, we discuss here initial guesses for general directrix cylinders.
[S2] presents a very useful compendium for Least Squares fitting for general testing, based on orthogonal distance to the analytical surface. In our case, we complement these algorithms with our Initial-Guess estimation for the Levenberg Marquardt algorithms in [S2].

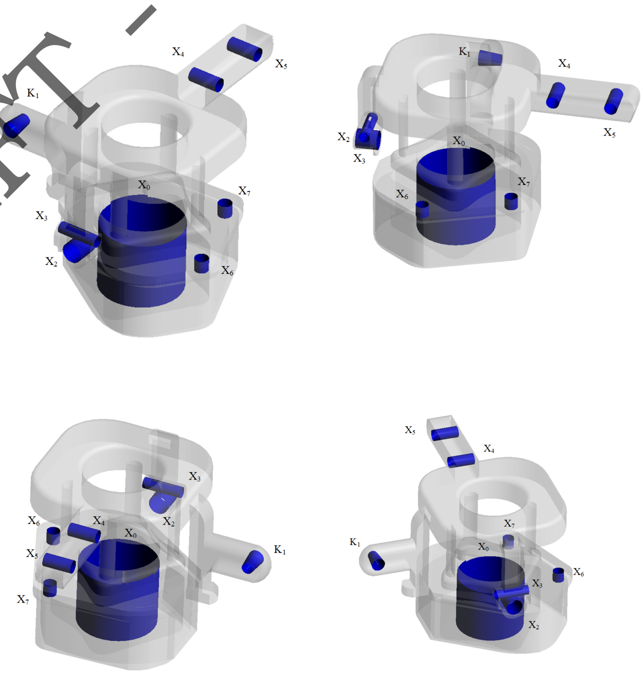

Figure 1: Workpiece.

3- Methodology

Fig. 1 displays a study case workpiece on which the tolerance assessment is tested. A Coordinate Measuring System (CMS) contact point sample is taken from the features: (1) Πp Bearing Resting Plane, (2) Cyl-1 Bearing Cylinder , (3) Cyl-2 Knuckle Cylinder and (4) Cn-1 Cone. Each one of these point samples triggers a Levenberg Marquardt (LM) optimal fitting, which estimates a general plane, cylinder, cylinder and cone, respectively, therefore rendering estimations of their geometrical components.

Entity Type	Analytic Primitives	Estimated Geometrical Components
Plane	Πp	plane pivot point pv
		plane normal vector np
Cylinder	Cyl-1	cylinder axis vector vA
		cylinder axis pivot pA
		cylinder cylinder radius r1
Cylinder	Cyl-2	cylinder axis vector vG
		cylinder axis pivot pE
		cylinder radius r2
Cone	Cn-1	cone axis vector $\boldsymbol{v_F}$
		cone apex pF
		cone angle β_1

Table 1. Initial Point Samples and Estimated Geometrical Components.

Fig. 2 shows the data flow of the Object Oriented code, which lends itself to be parallel. The statistical fit for analytical primitives Pp, Cyl-1, Cyl-2 and Cone-1 instances several geometric components for each one of them. For example, the fitting for the cone Cn-1 renders: (1) the cone axis vector, (2) cone angle, and (3) cone apex. Notice that the cone axis can be expressed as a 3D parametric line $\boldsymbol{L}(\ )$ ($\boldsymbol{L}(\alpha) = \boldsymbol{p_v} + \alpha * \boldsymbol{v}$) with $\boldsymbol{p_v}$ = cone apex and $\boldsymbol{v}$ = cone axis direction vector. Table 1 presents the geometric parameters that are extracted form the initial fit of the analytic primitives Plane, Cone and Cylinder.

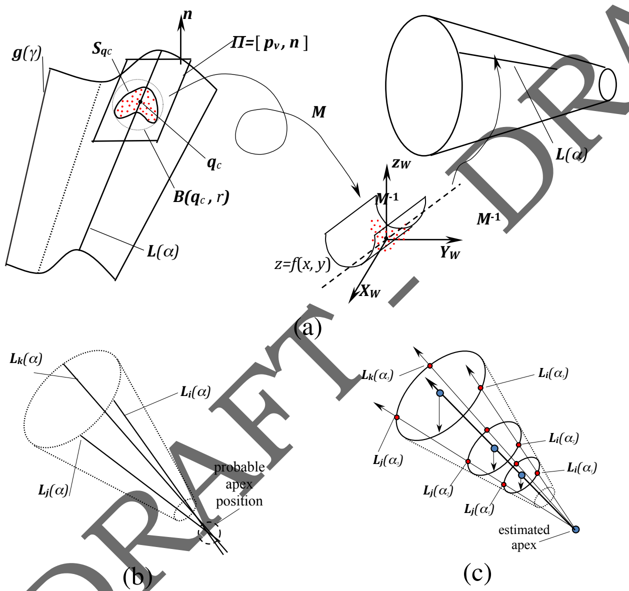

Figure 2: Initial Guess for Cone Fitting. ([RUIZ.2013])

Fig. 2 displays an initial method for initial estimation of cone parameters, prerequisite of the LM fitting ([RAA1]). Fig 2-a indicates that a generalized cone is a ruled surface. Any local neighbourhood may be rigidly transported (via $\boldsymbol{M}$) to the origin of $\boldsymbol{R^3}$ forming a local channel surface which has a direction of minimal (zero) curvature and a perpendicular direction of maximal curvature. The minimal curvature direction is back transformed via $\boldsymbol{M^{-1}}$, estimating the local generatriz $L(\alpha)$. Fig 2-b displays how the process is repeated for several neighborhoods of the cone, obtaining a set of cone generatrices $\{L_1(\alpha), L_2(\alpha), \ldots\}$ which approximately meet in the Apex of the cone. Fig. 2-c shows that each one of the generatrix lines $L_i(\alpha)$, can be re-parameterized to have its origin $\boldsymbol{p_v}$ in the cone apex. In these conditions, it is easy to generate a family of circles perpendicular to, and with centers lying on, the cone axis. Principal Component Analysis identifies the cone axis $\boldsymbol{v_F}$. The cone angle β_1 trivially follows.

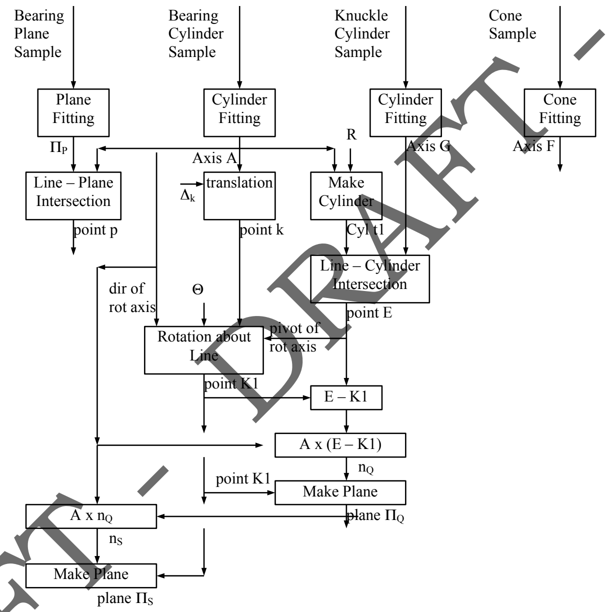

Figure 3: Data Flow Chart.

Fig 2-a indicates a similar strategy to identify a cylinder with general position in $\boldsymbol{R^3}$. In a cylinder, all the local $\boldsymbol{q_c}$ lines are supposed to hit the cylinder axis. Given any pair of lines $\boldsymbol{q_i}$ and $\boldsymbol{q_j}$, they cross (in general) without intersection in $\boldsymbol{R^3}$. The crossing point on each one of the ($\boldsymbol{q_i}$ vs. $\boldsymbol{q_j}$) pairs lies on the cylinder axis. This set of crossing points renders (via Principal Component Analysis) an initial guess for the cylinder axis. The cylinder radius trivially follows.

Fig 3. Shows an generalization of the fitting of analytic primitives based on the point samples. The data flow graph shows conceptually different processes, as follows: (1) Interrogations, in which an analytic form is interrogated for its components (e.g. given a plane, retrieve its normal vector). (2) Geometric transformations of given primitives by given parameters (e.g. quaternion rotation of a point about an axis by a given angle). (3) Creation of new analytic primitives from given parameters (e.g. create a plane from a pivot point and a normal vector). (4) Calculation of new geometric objects (e.g. vectors, points, lines) based on the existing ones. Notice that the graph so built contains also the possibility to *assess* whether a geometric relation (for example, a tolerance) is satisfied.

4- Results

Fig. 3 shows is a very limited subset (for the sake of brevity) of the actual calculation and assessment graph actually implemented in industrial level. The implemented system allowed, from the sampling of the initial 4 primitives, the generation of datums removed from the workpiece (Figs. 4 and 5). These datums, and the remaining part of the tolerance graph allowed in turn the assessment of more than 100 entities of interest in the worpiece evaluated. Fig. 5 shows a navigation scene in a Virtual Reality Modeling Language (VRML) derived file.

Fig. 5, the implemented system assesses a large set of primitives of the workpiece, building a partially virtual world from the fitting of 4 features (2 cylinders, 1 plane, 1 cone), selected by the manufacturing engineers. The enginners selected these features since those are the kernel of fixturing and machining of the workpiece.

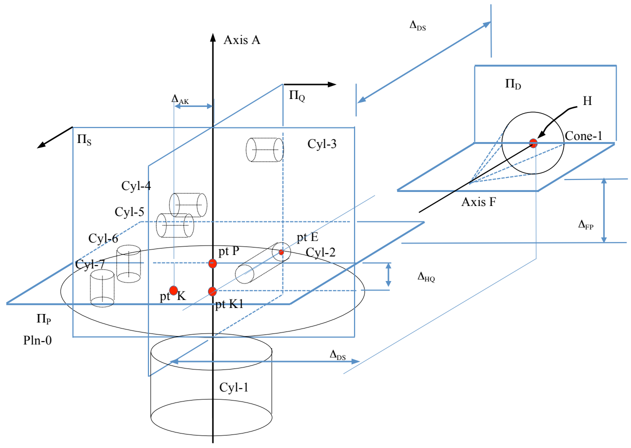

Figure 4: World Entities.

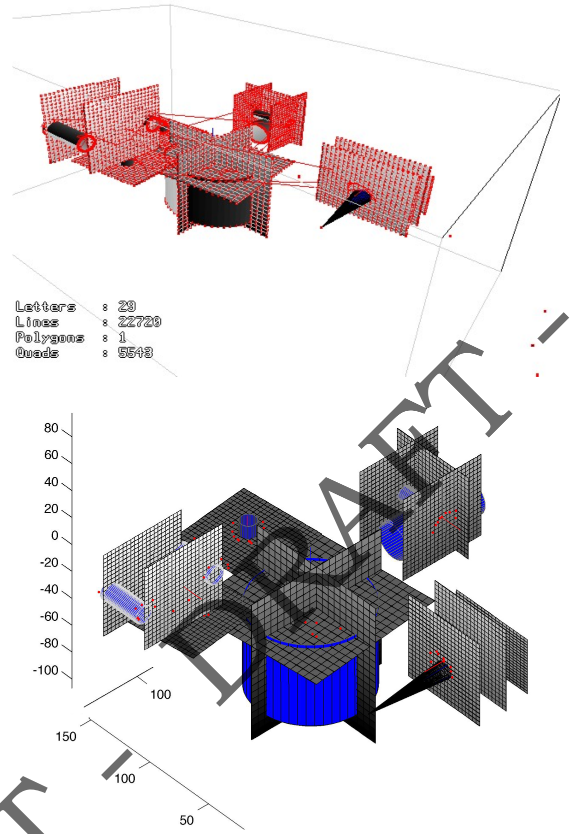

Figure 5. Recovered Entities.

5- Conclusions

This manuscript describes the implementation of an industrial system for the assessment of tolerances, based on a generalization of geometric constraints graphs. The graphs implemented include other types of edges, besides the geometric constraint ones, allowing for auxiliary constructs of virtual, remote features. These in turn allow for the assessment of a large set of tolerances on features-of-interest in the workpiece. The software was implemented using an Extended Object Oriented paradigm, which makes accessible the reconfiguration for the evaluation of other workpieces.

6- Acknowledgements

The authors wish to thank undergraduate students Daniel Burgos and Juan Jose Londoño for their incarnation of the CAD designs used in this article.

7- References

[RAA1] Oscar Ruiz, Santiago Arroyave, Diego Acosta. Fitting of Analytic Surfaces to Noisy Point Clouds. In American Journal of Computational Mathematics, ISSN Print: 2161-1203, ISSN Online: 2161-1211, Volume 3, Number 1A - Special issue on Computational Geometry. pages 18-26, 2013.

[DQ1] Jean-Yves Dantan, Ahmed-Jawad Qureshi. Worst-case and statistical tolerance analysis based on quantified constraint satisfaction problems and Monte Carlo simulation. In Computer-Aided Design, v. 41, 1-12, 2009.

[S1] Vijay Srinivasan. Computational Metrology for the Design and Manufacture of Product Geometry: A Classification and Synthesis. J. Comput. Inf. Sci. Eng. 7(1) : 3-9. 2006.

[SS1] Craig M. Shakarji, Vijay Srinivasan. Theory and Algorithms for Weighted Total Least-Squares Fitting of Lines, Planes, and Parallel Planes to Support Tolerancing Standards. J. Comput. Inf. Sci. Eng. 13(3), 031008. 2013.

[PSRS1] V. Portman; V. Shuster; Y. Rubenchik; Y. Shneor. Substitute Geometry of the Features of Size: Applications to Multidimensional Features. J. Comput. Inf. Sci. Eng. 7(1) : 52-65. 2006

[S2] Craig M. Shakarji. Least-Squares Fitting Algorithms of the NIST Algorithm Testing System. 103(6), J. Res. Natl. Inst. Stand. Technol. 633-641. 1998